



The potential antibacterial application of Mg-doped zinc oxide nanoparticles synthesized through sol-gel method

Roghayeh Shahriari, Mohammad Ghorbanpour*

Department of Chemical and Petroleum Engineering, University of Tabriz, Tabriz.

Received: 21 March 2024; Accepted: 11 June 2024

*Corresponding author email: Ghorbanpour@tabrizu.ac.ir

ABSTRACT

The current study introduces an uncomplicated approach to produce Mg-doped ZnO nanoparticles through the sol-gel method, eliminating the need for a washing procedure, and assessing its antibacterial properties. The characteristics of the nanoparticles were examined through advanced techniques such as scanning electron microscopy (SEM), X-ray diffraction (XRD), and UV-Vis diffuse reflectance spectroscopy. The resulting Mg-doped ZnO nanoparticles displayed a spherical morphology. The antibacterial activity of these nanoparticles was evaluated. Prepared ZnO had a hexagonal wurtzite crystal structure. The incorporation of Mg into ZnO led to a modification of its band gap from 3.23 eV for pure ZnO to 3.18 eV for doped ZnO. MgO has a wider band gap compared to ZnO, and by doping ZnO with Mg, the band gap of the resulting Mg doped ZnO particles can be adjusted. The results exhibited inhibition sizes of 7.7 mm and 6.1 mm against *E. coli* and *S. aureus*, respectively. Following Mg doping, the inhibition zone against *E. coli* and *S. aureus* increased to 8.3 mm and 9.1 mm, respectively. The decrease in band gap values could be the reason behind the enhanced bactericidal activity as it increases the likelihood of hydroxyl radical generation. The results clearly show that the Mg doping have positive effect on the antimicrobial effects against *E. coli* and *S. aureus* bacteria.

Keywords: Antibacterial activity, potential application, Sol-gel, Mg, doping, zinc oxide.

1. Introduction

Industries are currently making use of a variety of nanoparticles such as titanium dioxide, zinc oxide, copper oxide, magnesium oxide, silica dioxide, chromium oxide, nickel oxide, manganese oxide, and cobalt oxide, among others, because of their interesting properties and application [1-7]. Nanoparticles exhibit harmful effects on various microorganisms, successfully eradicating a variety of bacteria [8-10]. Zinc oxide nanoparticles, in particular, are a diverse type of semiconductor material with a broad band gap of 3.37 eV, high binding energy, excellent ultraviolet absorption capabilities, superior chemical stability, and a hexagonal wurtz-

ite structure [11]. In recent years, there has been a growing interest in utilizing zinc oxide (ZnO) in various nanomaterial applications, including gas sensors, photo-catalytic processes, dye-sensitized solar cells, antibacterial products, water purification systems, textiles, and food packaging [12]. ZnO also possesses antibacterial properties that are advantageous for pharmaceutical and biological uses [13,14]. The characteristics of ZnO are influenced by the defects present in the material, such as oxygen vacancies [15]. By introducing impurities into ZnO at different doping levels, it is possible to modify and enhance the properties of ZnO [16]. Alternatively, as evidenced in various studies, uti-

lizing doping techniques can result in significant alterations in the physical and chemical characteristics of ZnO nanoparticles, ultimately boosting their photocatalytic and antibacterial capabilities [17]. In recent times, there have been numerous efforts made to incorporate metal ions such as calcium, silver, copper, iron, and magnesium into the structure of photo-catalysts [18-20]. In the list of metals discussed, it was found that ZnO nanoparticles doped with Mg showed antibacterial properties. This is because Mg^{2+} ions can take the place of Zn^{2+} ions in the structure due to their similar sizes. This substitution causes the ZnO lattice to become distorted, creating oxygen or zinc vacancies [21]. As a result, there is an increase in the energy gap between the valence and conduction bands of ZnO. This leads to better absorption of light and the generation of more electron-hole pairs, ultimately improving the photocatalytic efficiency of the ZnO nanostructures [22]. For instance, Etacheri *et al.* (2012) have created magnesium-doped zinc oxide nanoparticles that utilize sunlight for photocatalysis. The band gap of these magnesium-doped zinc oxide samples can range from 3.3 to 3.75 eV [16]. The study conducted by Habibi-Yangjeh *et al.* (2014) demonstrated that the microwave-assisted synthesis of Mg-doped ZnO nanostructures resulted in exceptional photocatalytic performance. [23]. Ivetić *et al.* (2014) have shown that the addition of magnesium improves the effectiveness of ZnO nanoparticles in the process of breaking down alprazolam through

photocatalysis [24]. Chandraseka *et al.* (2020) in their recent study have successfully created magnesium-doped zinc oxide nanoparticles through a chemical precipitation process [16]. Their findings revealed that these doped ZnO nanoparticles exhibit remarkable antibacterial properties against *E. coli*. Additionally, the researchers observed that the band gap of the Mg-doped ZnO samples can range from 3.3 to 3.15 eV. Various chemical methods of synthesis are applied to synthesize nanostructured ZnO powders containing using hydrothermal [25], precipitation [16], sol-gel [26,27], layer-by-layer electrostatic assembly [28], and thermal decomposition [29] methods. The sol-gel method stands out as a preferred choice among various methods for nanoparticle synthesis, mainly due to its simplicity, high product purity, low processing temperature, easy doping capability, cost-effectiveness, and the ability to create uniform nanostructures suitable for mass production [27,30]. A common challenge encountered during nanoparticle synthesis is the meticulous washing process needed to eliminate byproducts and contaminants, which often leads to smaller particle loss. This research deviated from conventional sol-gel methodologies by skipping the washing step. The study focused on producing ZnO nanoparticles with Mg doping using the sol-gel method. It aims to investigate how Mg doping affects the structural, optical, and antibacterial properties of ZnO. The results include an examination of characterization techniques and the antibacterial

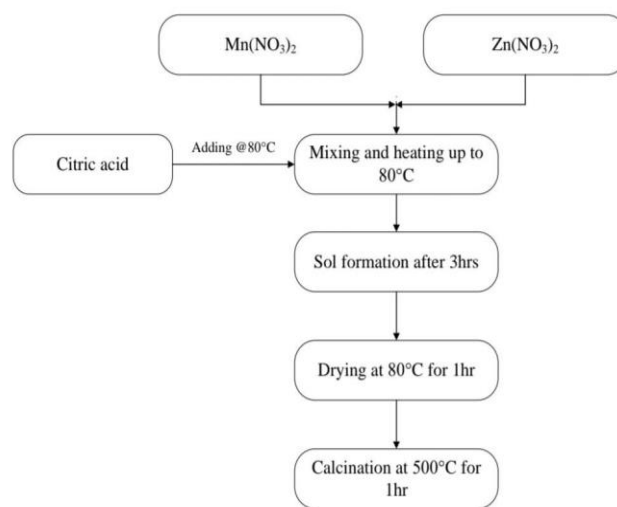


Fig. 1- Schematic of synthesis method.

effectiveness against *E. coli* and *S. aureus*.

2. Material and methods

2.1. Chemicals

The zinc nitrate (98%) was obtained from Merck Co, along with the magnesium nitrate (99%) and citric acid (98%) used in the experiment. The chemicals were all purchased in their pure form and were not subjected to any additional purification processes. The nutrient agar used in the experiment was also obtained from Merck Co.

2.2. Synthesis procedure

Citric acid was carefully added in small drops to a mixture of $Zn(NO_3)_2$ and $Mg(NO_3)_2$. The molar ratio of metal ions to Citric acid was maintained at 1:1. The molar ratio of Mg^{2+} to Zn^{2+} was also 1:1. The temperature of the solution was then slowly raised to 60 °C using a water bath. Over the course of an hour, the solution transformed from a liquid to a hydrogel. The resulting gel was subsequently dried at 80 °C for 48 hours in a vacuum oven. The resulting xerogel contained evenly distributed magnesium ions bound by citric acid. The xerogel was then subjected to calcination at 500 °C for 1 hour. The synthetic method is illustrated schematically in Figure 1.

2.3. Characterization

A LEO 1430VP device (Germany) was employed for scanning electron microscopy. Additionally, a Philips PW 1050 diffractometer from The Netherlands was used to conduct powder X-ray diffraction studies. Furthermore, powder samples were examined using Diffuse Reflectance UV-Vis Spec-

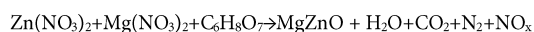
troscopy (DR UV-Vis) across a wavelength range of 200–800 nm. This analysis was carried out using a spectrophotometer from Scinco S4100 based in South Korea. To evaluate the size and distribution of nanoparticles, DLS analysis (Horiba, SZ-100) was employed.

2.4. Antibacterial activity

The study aimed to assess the antibacterial properties of undoped and Mg-doped zinc oxide nanoparticles against *E. coli* and *S. aureus* bacteria through an agar diffusion test. Nutrient agar plates were inoculated with 100 μ L of bacterial suspensions. Discs loaded with 0.05 g of samples and measuring 0.5 cm in diameter were placed on the agar surface and incubated at 37 °C for 24 hours under UV light (Philips, 4W). The presence of inhibition zones, indicating the suppression of bacterial growth, was visually examined.

3. Results and discussion

In the sol-gel method utilized in the present study, the reaction proceeds as follows:



One important aspect of this chemical reaction is that all resulting substances, with the exception of MgZnO, exist in the form of gases, making it easy to remove and separate them from the main product. As a result, there is no need for a washing process to eliminate any leftover materials.

The SEM images in Figure 2 display the differences between undoped and magnesium-doped Zinc Oxide. It is evident that the introduction of

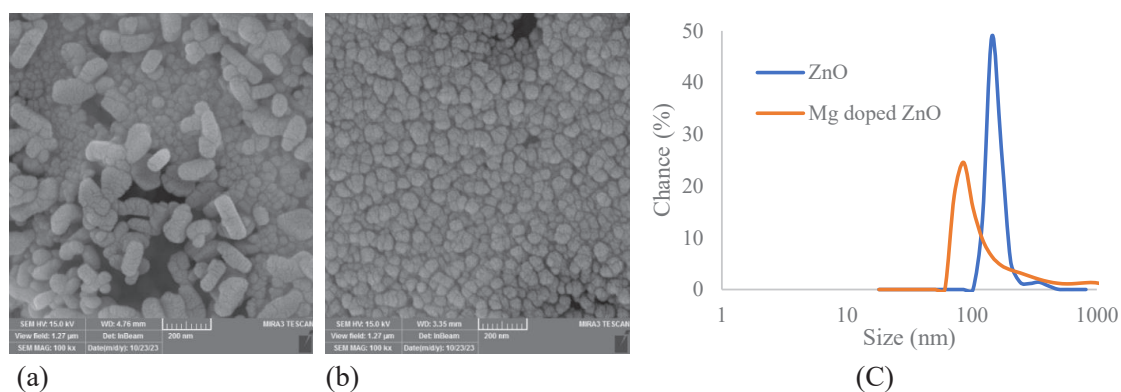


Fig. 2- SEM image of undoped (a) and Mg doped ZnO (b) and DLS results (C).

magnesium dopant results in a noticeable decrease in the average particle size. This observation is consistent with previous research [31]. In the case of undoped ZnO nanoparticles, two distinct types of grains were observed: one type consisting of larger oval-shaped grains, and the other made up of smaller spherical grains. However, after magnesium doping, the larger grains disappeared. This can be attributed to the magnesium ions disrupting the ZnO crystal lattice, thus impeding crystal growth. After analyzing the data with Dynamic Light Scattering (DLS), it was noticed that the average size of ZnO particles decreased significantly from around 161.2 nm to 93.4 nm after doping, as illustrated in figure 2c. In a study conducted by Kılınc *et al.* (2010), they created Mg_{0.04}Zn_{0.96}O powder through the sol-gel method, utilizing solutions of organometallic compounds of Mg and Zn. They successfully achieved particle sizes ranging from 60 to 200 nm [26].

The samples were analyzed using powder X-ray diffraction to determine their level of purity, structure, and size of crystallites. The XRD patterns of both the ZnO and ZnO samples doped with Mg are displayed in Figure 3. In all diffractograms, prominent XRD peaks were observed at around $2\theta = 31.61^\circ$, 34.31° , and 36.11° [32]. All of these diffraction peaks were in good agreement with the hexagonal wurtzite phase of ZnO (JCPDS No. 36-1451). After addition of Mg, the wurtzite characteristics of the nanoparticles remain consistent. The differ-

ence is the formation of one new peak at round $2\theta = 42.78^\circ$, which indicates the formation of a new MgO phase. According to Wu *et al.* (2013) the limitation concentration of Mg dopant in ZnO structure is less than 15% [33]. This suggests that incorporating more than 15% Mg dopant into the ZnO structure may lead to a change in the phase transition, resulting in a new phase (MgO) at around 2θ value of 42.78° . Finally, The variation in peak intensity and position in the XRD pattern indicate a successful integration of Mg into the ZnO lattice.

The impact of magnesium (Mg) doping on the optical properties was investigated by the UV-Vis DRS in the wavelength range of 200-800 nm. The absorption spectra are presented in Figure 4. It was observed that the absorption peak of pure ZnO occurred around 390 nm, whereas the Mg-doped ZnO showed a red shift in its absorption spectrum. The Mg-doped ZnO exhibited increased absorbance in the 400-800 nm range compared to the pure ZnO. The calculated band gap energy was found to be 3.23 eV for pure ZnO and 3.18 eV for Mg-doped ZnO. The Mg-doped ZnO demonstrated lower band gap energy levels than the pure ZnO. The size of the crystallites and the band gap play crucial roles in determining the properties of semiconductor materials. The study indicated that the introduction of Mg into ZnO can alter both the structural and optical properties of the synthesized nanoparticles [16]. Furthermore, the obtained band gap energy value of 3.18 eV for Mg-doped

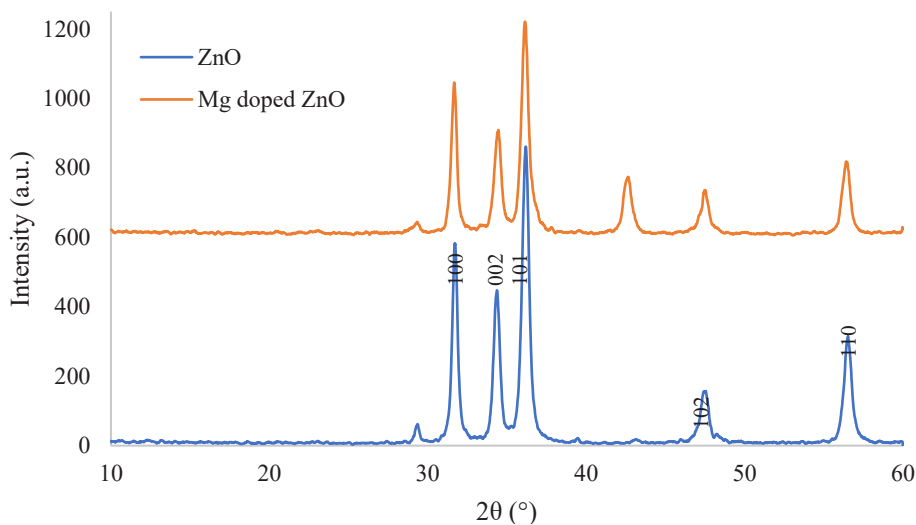


Fig. 3- XRD patterns of undoped and Mg doped ZnO.





zinc oxide nanoparticles aligns with findings from previous studies that utilized more complex preparation techniques [22,34].

3.1. Antibacterial activity screening

The study on the antimicrobial properties of the samples was conducted using the malt-agar method against *E. coli* and *S. aureus*. The results are depicted in Table 1. In the petri dishes containing *E. coli* and *S. aureus*, the undoped samples exhibited inhibition ring sizes of 7.7 mm and 6.1 mm, respectively. Zinc oxide nanoparticles exhibit bactericidal activity through various means, including adsorption onto bacterial surfaces, creation of intermedi-

ates, and electrostatic interactions. These nanoparticles possess the capability to target multiple areas within bacterial cells, primarily affecting the cytoplasmic membrane. The impact on other cellular structures is considered to be secondary to the membrane disruption [35]. Following Mg doping, the inhibition ring sizes against *E. coli* and *S. aureus* increased to 8.3 mm and 9.1 mm, respectively. The results clearly show that the Mg doping have positive effect on the antimicrobial effects against *E. coli* and *S. aureus* bacteria. The enhancement of antimicrobial efficacy in doped samples correlates with the production of Reactive Oxygen Species (ROS), a phenomenon influenced by their energy band gap.

Table 1- The Antibacterial activity of Undoped and Mg doped ZnO

	Undoped ZnO		Mg doped ZnO	
	Photograph	Inhibition sizes (mm)	Photograph	Inhibition sizes (mm)
<i>E. coli</i>		7.7		8.3
<i>S. aureus</i>		6.1		9.1

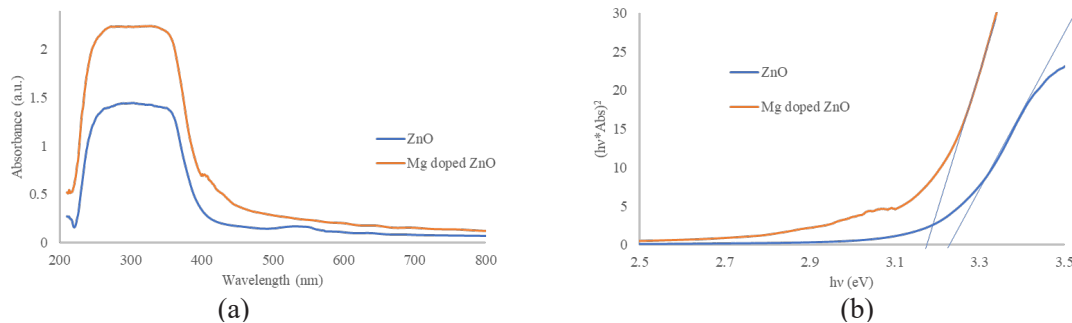


Fig. 4- UV-Vis DRS spectroscopy of undoped (a) and Mg doped ZnO (b)

The creation of valence band vacancies through a photochemical process leads to the synthesis of hydroxide radicals and superoxide radicals as ROS. Illustrated in figure 3b, the energy band gap dwindled upon the addition of Mg dopant, potentially due to the flaws triggered by substituting Mg^{2+} for Zn^{2+} and the simultaneous integration of Mg possessing distinct electronegativity and ionic radius into structure of ZnO. This, in turn, boosts both the oxygen vacancies and electron density, signifying the efficient production of ROS. Consequently, the Mg-infused ZnO showcased elevated antimicrobial efficacy [36]. Additionally, the unique surface and interface properties of the nanoparticles might influence their capacity to attract and repel bacteria, resulting in varying degrees of antibacterial effectiveness [37].

4. Conclusion

The sol-gel method was utilized effectively to

produce Mg-doped ZnO nanoparticles. Based on the SEM images, it is clear that the addition of magnesium dopant leads to a significant reduction in the average particle size, dropping from approximately 161.2 nm to 93.4 nm. The synthesized ZnO possessed a hexagonal wurtzite crystal structure. The introduction of magnesium into ZnO resulted in a modification of its energy band gap from 3.23 eV for pure ZnO to 3.18 eV for doped ZnO. The findings demonstrated inhibition zones of 7.7 mm and 6.1 mm against *E. coli* and *S. aureus*, respectively. Following the incorporation of Mg, the inhibition zones against *E. coli* and *S. aureus* increased to 8.3 mm and 9.1 mm, respectively. The decrease in band gap values could be the reason behind the enhanced bactericidal activity as it increases the likelihood of hydroxyl radical generation. The results clearly indicate that magnesium doping has a beneficial impact on the antimicrobial efficacy against *E. coli* and *S. aureus* bacteria.

References

1. Asghari R, Safavi MS, Khalil-Allafi J. A facile and cost-effective practical approach to develop clinical applications of NiTi: Fenton oxidation process. *Transactions of the IMF*. 2020;98(5):250-7.
2. Mozetič M. Surface Modification to Improve Properties of Materials. *Materials (Basel)*. 2019;12(3):441.
3. Safavi MS, Khalil-Allafi J, Ahadzadeh I, Walsh FC, Visai L. Improved corrosion protection of a NiTi implant by an electro-deposited HAp-Nb2O5 composite layer. *Surface and Coatings Technology*. 2023;470:129822.
4. Shokri N, Safavi MS, Etmannanfar M, Walsh FC, Khalil-Allafi J. Enhanced corrosion protection of NiTi orthopedic implants by highly crystalline hydroxyapatite deposited by spin coating: The importance of pre-treatment. *Materials Chemistry and Physics*. 2021;259:124041.
5. Alatabe, M.J.A., 2023. Ultraviolet Radiation for Phenol Removal from Aqueous Solutions by Copper Oxide Nanoparticles in Advanced Oxidation Process. *Iran. J. Chem. Chem. Eng. Research Article Vol*, 42(2).
6. Katzer JR. Catalytic Oxidation of Phenol in Aqueous Solution over Copper Oxide. *Industrial & Engineering Chemistry Fundamentals*. 1978;17(3):234-.
7. Yaqoob AA, Ahmad H, Parveen T, Ahmad A, Oves M, Ismail IMI, et al. Recent Advances in Metal Decorated Nanomaterials and Their Various Biological Applications: A Review. *Front Chem*. 2020;8:341-.
8. Hakimi, B., Ghorbanpour, M. and Feizi, A., 2018. A comparative study between photocatalytic activity of ZnO/bentonite composites prepared by precipitation, liquid-state ion exchange and solid-state ion exchange methods. *Journal of Water and Environmental Nanotechnology*, 3(3), pp.273-278.
9. Gilani S, Ghorbanpour M, Parchehbaf Jadid A. Antibacterial activity of ZnO films prepared by anodizing. *Journal of Nanostructure in Chemistry*. 2016;6(2):183-9.
10. Lotfiman S, Ghorbanpour M. Antimicrobial activity of ZnO/silica gel nanocomposites prepared by a simple and fast solid-state method. *Surface and Coatings Technology*. 2017;310:129-33.
11. Jiang Z, Liu B, Yu L, Tong Y, Yan M, Zhang R, et al. Research progresses in preparation methods and applications of zinc oxide nanoparticles. *Journal of Alloys and Compounds*. 2023;956:170316.
12. Gadewar M, Prashanth GK, Ravindra Babu M, Dileep MS, Prashanth PA, Rao S, et al. Unlocking nature's potential: Green synthesis of ZnO nanoparticles and their multifaceted applications – A concise overview. *Journal of Saudi Chemical Society*. 2024;28(1):101774.
13. Malhotra SPK, Mandal TK. Zinc oxide nanostructure and its application as agricultural and industrial material. *Contaminants in Agriculture and Environment: Health Risks and Remediation: Agro Environ Media - Agriculture and Environmental Science Academy, Haridwar, India; 2019*. p. 216-26.
14. Hakimi, B., Ghorbanpour, M. and Feizi, A., 2018. ZnO/bentonite nanocomposites prepared with solid-state ion exchange as photocatalysts. *Journal of Ultrafine Grained and Nanostructured Materials*, 51(2), pp.139-146.
15. Liu J, Wang Y, Ma J, Peng Y, Wang A. A review on bidirectional analogies between the photocatalysis and antibacterial properties of ZnO. *Journal of Alloys and Compounds*. 2019;783:898-918.
16. Chandrasekar LB, Gnaneswari MD, Karunakaran M. Synthesis, characterization and anti-bacterial activity of Mg and Ba-doped ZnO Nanoparticles. *Journal of Materials Science: Materials in Electronics*. 2020;31(22):20270-6.
17. Qi K, Cheng B, Yu J, Ho W. Review on the improvement of the photocatalytic and antibacterial activities of ZnO. *Journal of Alloys and Compounds*. 2017;727:792-820.
18. Shenoy RUK, Rama A, Govindan I, Naha A. The purview of doped nanoparticles: Insights into their biomedical applications. *OpenNano*. 2022;8:100070.
19. Madadi M, Ghorbanpour M, Feizi A. Preparation and characterization of solar light-induced rutile Cu-doped TiO₂ photocatalyst by solid-state molten salt method. *DESALINATION*

- AND WATER TREATMENT. 2019;145:257-61.
20. Madadi M, Ghorbanpour M, Feizi A. Antibacterial and photocatalytic activity of anatase phase Ag-doped TiO₂ nanoparticles. *Micro & Nano Letters*. 2018;13(11):1590-3.
 21. El Hamidi A, El Mahboub E, Meziane K, El Hichou A, Almagoussi A. The effect of electronegativity on optical properties of Mg doped ZnO. *Optik*. 2021;241:167070.
 22. Chen C, Yu W, Liu T, Cao S, Tsang Y. Graphene oxide/WS₂/Mg-doped ZnO nanocomposites for solar-light catalytic and anti-bacterial applications. *Solar Energy Materials and Solar Cells*. 2017;160:43-53.
 23. Nouri H, Habibi-Yangjeh A. Microwave-assisted method for preparation of Zn_{1-x}Mg_xO nanostructures and their activities for photodegradation of methylene blue. *Advanced Powder Technology*. 2014;25(3):1016-25.
 24. Ivetić TB, Dimitrievska MR, Finčur NL, Đačanin LR, Gúth IO, Abramović BF, Lukić-Petrović SR. Effect of annealing temperature on structural and optical properties of Mg-doped ZnO nanoparticles and their photocatalytic efficiency in alprazolam degradation. *Ceramics International*. 2014;40(1):1545-52.
 25. Gerbreders V, Krasovska M, Sledevskis E, Gerbreders A, Mihailova I, Tamanis E, Ogurcovs A. Hydrothermal synthesis of ZnO nanostructures with controllable morphology change. *CrystEngComm*. 2020;22(8):1346-58.
 26. Kılınc, N., Arda, L., Öztürk, S. and Öztürk, Z.Z., 2010. Structure and electrical properties of Mg-doped ZnO nanoparticles. *Crystal Research and Technology*, 45(5), pp.529-538.
 27. Zheng K, Boccaccini AR. Sol-gel processing of bioactive glass nanoparticles: A review. *Advances in Colloid and Interface Science*. 2017;249:363-73.
 28. Etacheri V, Roshan R, Kumar V. Mg-Doped ZnO Nanoparticles for Efficient Sunlight-Driven Photocatalysis. *ACS Applied Materials & Interfaces*. 2012;4(5):2717-25.
 29. Suwanboon S, Amornpitoksuk P, Sukolrat A. Dependence of optical properties on doping metal, crystallite size and defect concentration of M-doped ZnO nanopowders (M = Al, Mg, Ti). *Ceramics International*. 2011;37(4):1359-65.
 30. Bokov D, Turki Jalil A, Chupradit S, Suksatan W, Javed Ansari M, Shewael IH, et al. Nanomaterial by Sol-Gel Method: Synthesis and Application. *Advances in Materials Science and Engineering*. 2021;2021:1-21.
 31. Wang C, Chen Z, He Y, Li L, Zhang D. Structure, morphology and properties of Fe-doped ZnO films prepared by facing-target magnetron sputtering system. *Applied Surface Science*. 2009;255(15):6881-7.
 32. Karthikeyan B, Pandiyarajan T. Simple room temperature synthesis and optical studies on Mg doped ZnO nanostructures. *Journal of Luminescence*. 2010;130(12):2317-21.
 33. Wu Y, Yun J, Wang L, Yang X. Structure and optical properties of Mg-doped ZnO nanoparticles by polyacrylamide method. *Crystal Research and Technology*. 2013;48(3):145-52.
 34. Suwanboon S, Amornpitoksuk P, Sukolrat A. Dependence of optical properties on doping metal, crystallite size and defect concentration of M-doped ZnO nanopowders (M = Al, Mg, Ti). *Ceramics International*. 2011;37(4):1359-65.
 35. Mendes CR, Dilarri G, Forsan CF, Sapata VdMR, Lopes PRM, de Moraes PB, et al. Antibacterial action and target mechanisms of zinc oxide nanoparticles against bacterial pathogens. *Sci Rep*. 2022;12(1):2658-.
 36. Adesoye S, Al Abdullah S, Nowlin K, Dellinger K. Mg-Doped ZnO Nanoparticles with Tunable Band Gaps for Surface-Enhanced Raman Scattering (SERS)-Based Sensing. *Nanomaterials (Basel)*. 2022;12(20):3564.
 37. Pradeev Raj K, Sadaiyandi K, Kennedy A, Sagadevan S, Chowdhury ZZ, Johan MRB, et al. Influence of Mg Doping on ZnO Nanoparticles for Enhanced Photocatalytic Evaluation and Antibacterial Analysis. *Nanoscale Res Lett*. 2018;13(1):229-.